

# Segmentation of Moving Objects in SAR-MTI Data

K. Schulz\*, U. Soergel\* and U. Thoennessen\*  
FGAN-FOM Forschungsinstitut für Optronik und Mustererkennung  
Gutleuthausstr. 1, D-76275 Ettlingen, Germany

## ABSTRACT

The SAR processing is optimized for motionless scenes. Moving objects cause artifacts like blurring or azimuth displacement in case of parallel or radial velocity components respectively. With along-track interferometry (SAR-MTI) even very slow radial velocities can be measured by the phase differences. Unfortunately, the phase information is often severely disturbed, depending on a insufficient signal to noise ratio. In this paper we refer to investigations to stabilize and improve the SAR-MTI velocity data. Reliability is enhanced by a combined exploitation of phase and intensity. After speckle filtering a binary mask is generated from the intensity data to fade out regions with insufficient signal to noise ratio, like regions with low backscattering coefficient. In a next step for every point in the intensity image the radial velocity is calculated by the phase difference of two channels. This image of velocities is masked with the binary mask derived from the intensity image. A region growing process is initiated in the velocity image to identify connected regions in the image with similar velocity. By this process we get first hints for moving objects. The approach was applied to images with slow moving cargo ships inside and nearby locks. The cargo ships are segmented and described by a simple model. Only cargo ships with a minimum velocity which match the longitudinal and transversal extension features of the model are concerned in further processing. For every object a weighted average velocity is calculated. This mean velocity could be used to correct the position of the identified cargo ship in the image. The results are compared to an aerial image acquired at the same time as the SAR images.

**Keywords:** SAR-MTI, along-track interferometry, SAR interferometry, detection of ground targets, segmentation

## 1. INTRODUCTION

A typical application of interferometric SAR (InSAR) is the measurement of the terrain elevation (DEM) in the observed scene. InSAR is using two SAR images taken from antennas at slightly different locations for DEM estimation. The antennas are located perpendicular to the flight direction. Especially for airborne systems a further interesting application is possible – detection of moving ground objects with antennas positioned parallel to the flight direction (along-track interferometry, figure 1b). In both cases the images taken by an interferometric SAR system are processed coherently to obtain fine resolution information regarding the height or velocity of scene objects. For elevation estimation a multi-pass InSAR measurement may be used, assuming that the terrain will not change during the period between two passes. In remote sensing across-track interferometry in multi and single pass modus is frequently used to derive digital elevation models (DEM) of the earth surface and is described elsewhere [1, 2, 3].

For the interferometric determination of ground object velocities a single pass along-track measurement is required. This results in a higher demand on the hardware equipment (two antennas, two receiver channels, two sets of A/D converters, etc.). Additionally, for the detection and segmentation of moving objects on the ground or water surface a high spatial resolution is crucial. The identification and velocity estimation for single objects is limited to systems which resolve the objects not only as point scatterers. Nowadays mainly airborne SAR systems have the ability for this purpose. The main field of investigation concerning across-track interferometry is regarding the measurement of radial velocity fields to identify ocean surface or coastal currents e. g. [4, 5, 6, 7]. Nevertheless number of available high resolution SAR-systems with interferometric capabilities is increasing, and offers an additional way for the surveillance of slow traffic streams.

The height or the velocity information is proportional to the phase differences of the complex SAR images. Especially in areas with low SNR respectively poor coherence the phase information is severely disturbed. Hence, the noise component has to be removed or at least significantly reduced before further analysis. This smoothing is frequently done with *iconic* – pixel based – filtering, e.g. reduction of the noise variance by averaging the signal with a sliding square window or by

\*E-mail: {schulz,soe,thoe}@fom.fgan.de; phone: ++49 07243 992 129; fax: ++49 07243 992 299; <http://www.fgan.de>;  
FGAN-FOM, Research Institute for Optronics and Pattern Recognition, Gutleuthausstr. 1, D-76275 Ettlingen, Germany

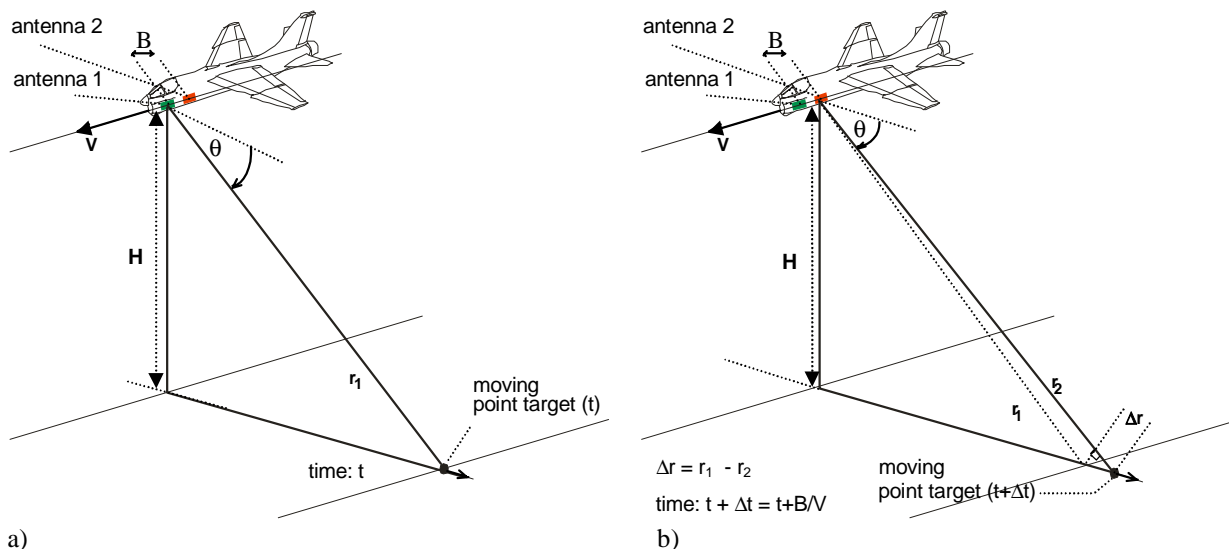


Figure 1: Geometry along-track interferometry

adding multiple independent looks. Unfortunately, filtering results in a reduced geometric resolution and signal jumps at object boundaries are blurred.

The smoothing of edges can be reduced by using anisotropic windows for the averaging, choosing the window with the lowest variance [8]. Other methods base on statistical modeling of sensor and scene [9]. With bayesian inference the data is restored to a configuration which approximates best the actual measured data [10, 11].

In this paper we propose a combined iconic and symbolic (model-based) approach to restore the phase differences, with a joined analysis of the phase and the intensity information. Methods, which were proposed for the semantic modeling of man-made objects in aerial imagery [12, 13], are adapted to SAR-MTI. Structural image analysis results in a symbolic description of the scene objects and their dependencies. Such a scene description is usually derived either with production nets or semantic nets. Starting with primitive objects, like short lines, more complicated objects are assembled, according to a set of rules. Besides the rules, hierarchical models of typical objects have to be provided a priori for this synthesis. The choice of suitable models and features can be supported by context knowledge. The models, rules, context knowledge, primitive and assembled objects are stored in a knowledge base.

The approaches are similar for InSAR and SAR-MTI data. The basic idea for InSAR data is already described in [14, 15]. They differ only due to the different nature of the expected objects, like roads and buildings or cargo ships respectively. In both cases a combined segmentation in the phase differences and intensities is carried out, to detect areas containing candidates for objects. Afterwards, the phase differences are smoothed, depending on the class of the object. In this step the phase differences are weighted with their related intensity or coherence value.

The task discussed in this paper is, to identify slowly moving cargo ships on inland waterways, which are entering or leaving the area in the vicinity of a lock. In every country there exist specific rules limiting the extensions of cargo ships using the waterways. Furthermore the velocities have to be in a well defined and comparatively low range. So the surveillance of the environment of locks is an interesting task. Our proposal deals with the problem to observe slowly moving traffic streams with an airborne SAR working in along-track modus.

The paper is organized as follows. First, we introduce in chapter 2 the experimental setup and processing for the across-track interferometry data. Our approach for modeling and segmentation of scene objects is described chapter 3. The subsections of this chapter includes the modeling of the scene objects and describes the segmentation approach. First results are presented in chapter 4. Chapter 0 gives a short summary and assessment of the achieved results with an outlook on further evaluation tasks.

## 2. ALONG-TRACK-INTERFEROMETRY

### 2.1 Experimental Setup

The data were recorded by the airborne AER-II experimental multi-channel SAR system of FGAN. This system has been tested in several measurement campaigns on board of a Transall C-160 airplane and is equipped with a phased array antenna and several receiver channels. The center frequency of this X-band system is 10 GHz with bandwidth of 160 MHz. The ground resolution achieves a spacing of approximately 1m x 1m. The system is described in detail elsewhere [16, 17].

### 2.2 Processing of Along-Track Interferometry Data

SAR along-track interferometry takes benefit from the coherent measurement principle. In a single pass system, two SAR signals  $s_1 = a_1 \cdot e^{j\phi_1}$  and  $s_2 = a_2 \cdot e^{j\phi_2}$  are received from two antennas with phase centers displaced by the baseline distance B along the flight direction [18, 19]. The signals received by the two antennas represent samples of the scene at intervals of time separated by  $\delta t = B/V$ , where V is the carrier velocity [5]. The phase of the interferogram calculated by multiplying the signal from the first antenna with the complex conjugated signal of the second antenna

$$S = s_1 \cdot s_2^* = a_1 \cdot a_2 \cdot e^{j\Delta\phi}, \quad (1)$$

carry information on the object displacement towards the system over the time interval  $\Delta t$  and leads to

$$v_{\text{rad}} = \frac{\lambda}{2\pi} \cdot \frac{V}{B \cdot \cos(\theta)} \cdot \Delta\phi, \quad (2)$$

for the ground velocity in radial direction with wavelength  $\lambda$ , carrier velocity V and depression angle  $\theta$  (Fig. 1.1). The phase difference  $\Delta\phi$  is unambiguous in  $]-\pi, \pi]$  only. The system parameters  $\lambda=0.03$  m,  $V= 88.6$  m/s and  $B=0.57$  m leads to an unambiguous velocity interval in the range of  $\pm 10.3$  km/h. This very small unambiguous velocity band indicates the sensitivity to small velocity but it leads to a difficult phase unwrapping problem, because of the fact that we can not assume steady and broad velocity changes in the scene.

## 3. APPROACH: MODELING AND SEGMENTATION OF SCENE OBJECTS

The presented approach of a combined evaluation of intensity and phase information presume that only image areas, which show a significant high intensity are suitable for calculations of reliable velocity values. Assuming that high intensities are correlated with high SNR, image areas with low intensities are masked before further processing.

The workflow of the evaluation process for SAR-MTI data is illustrated in Figure 2.

The result of this preliminary segmentation process is stored in a knowledge base. The SAR raw data processing provides complex values from two channels, which are used to calculate the corresponding intensity, height or velocity respectively, and to estimate the coherence. The approach consists of a combination of straightforward segmentation and rule based reconstruction of complex objects. We take benefit of the fact that object features appear different in the intensity and phase information. Hence, a combined analysis improves the reconstruction quality, due to accumulation of hints to objects in both channels. The information exchange is bi-directional. The parameters of the segmentation process are adjusted by information which are stored in the knowledge base like context information and object information resulting from the implemented model of the object (Figure 2). The modeling process of the scene objects is described in subsection 3.1. First a segmentation of primitive objects is carried out. For each of these objects a feature vector is calculated. Suitable features either relate to geometric segment properties - for example length, width, compactness, elongation and rectangularity - or to radiometric properties, like mean and variance of intensity. With a given set of rules, which are derived from the models of the objects, the primitives are classified to be an instance of one of the modeled object classes. In a second step, more complex objects are assembled from the set of regions, with a rule-driven evaluation.

The phase differences can now be restored for each object separately. The information about the object extension allows to determine a mean phase difference

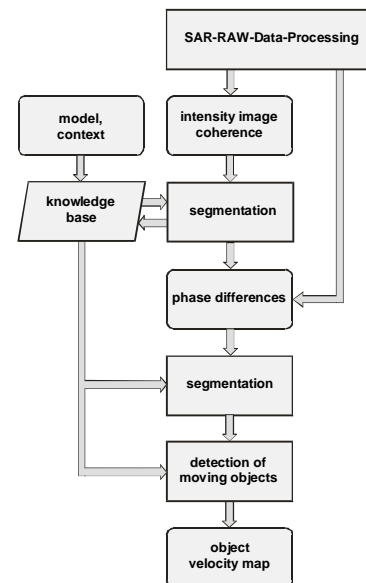


Figure 2: work flow diagram for the calculation of the object velocities

Feature	Minimum	Maximum
length	38,5 m	110,0 m
width	5,0 m	20,0 m
draught	2,0 m	3,0 m
load capacity	220 t	3000 t
velocity	0.7 km/h	12 km/h

by a simple averaging process over all values inside the object boundaries. The averaging process should be carried out on the original complex data or directly on the phase values with suitable weighting factor. Because of its dependency to the SNR, the coherence and the intensity were tested as weighting factor for this smoothing step.

### 3.1 Modeling of moving cargo ships

To identify slowly moving cargo ships on inland waterways, which are entering or leaving the area in the vicinity of a lock, a segmentation task was developed, which is supported by model based knowledge. In every country exist specific rules limiting the extensions of cargo ships using the waterways. Also the velocities are in a well defined and comparatively low range.

So a simple 2D model is used to detect cargo ships in the scenery. Due to the model of the searched objects, constraints are formulated concerning form features and the velocity. The searched objects are characterized by the features minimum area, and a minimum compactness. Furthermore the object form should have a characteristic ratio of width to length of the main axes, and the minimum and the maximum value for the main axes should be in a specific interval. For example the length of a cargo ships we are looking for is in the range of 38.5 m and 110 m. Because of the danger of bank damaging the allowed velocities are restricted and should not be higher than 12 km/h. It can be assumed that cargo ships entering and leaving the lock will not have the maximum allowed speed. Table 1 gives a short overview of main characteristics of the searched objects. The segmented objects are rigid and they have a constant velocity, different from zero over the whole object surface. It is assumed, that the phase differences of clutter (stationary image background) is assumed to be zero. Additionally we could formulate some conditions concerning the topological relationship between the searched object and their vicinity, e. g. cargo ships can only be located on waterways.

### 3.2 Segmentation of scene objects

The segmentation process should identify regions in the phase image, which are connected and which have a similar phase difference or velocity respectively. So for the segmentation, a region growing method is applied [14]. Regions are grown by attempting to merge as many adjacent pixels as possible with the constraint, that the difference between each phase value is less than a threshold. This measure is adaptively adjusted depending on the uniformity of the region, so as a region becomes less uniform its growth is limited (see Levine and Shaheen [14]). Because of the heavily distortion by the noise, the position of the ships in the phase image are difficult to identify. The phase image was masked by binary mask derived from intensity image. All values with lower intensities as 27 dB calculated by the maximum intensity value were masked. Figure 5c shows the binary mask which mainly separates the water ways from the land. By a simple multiplication of the binary image with the velocity field derived by the phase differences we get the image shown in Figure 6a. The region growing process is started in the masked phase image and results in more than 700 extracted region objects.

For each region a set of features is calculated which describes the form and the radiometric properties of the extracted objects. To this set of objects we apply a rule system characterizing the searched objects. The result is a set of hypotheses fulfilling the conditions derived by our object model.

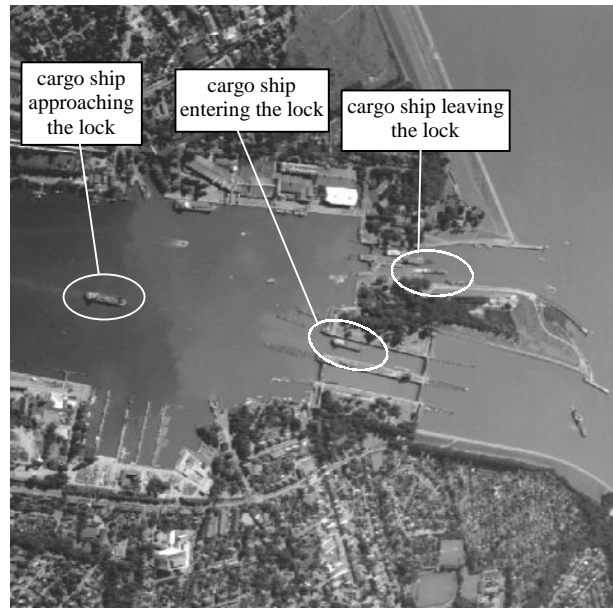


Figure 3: Aerial image acquired at the same time as the SAR images

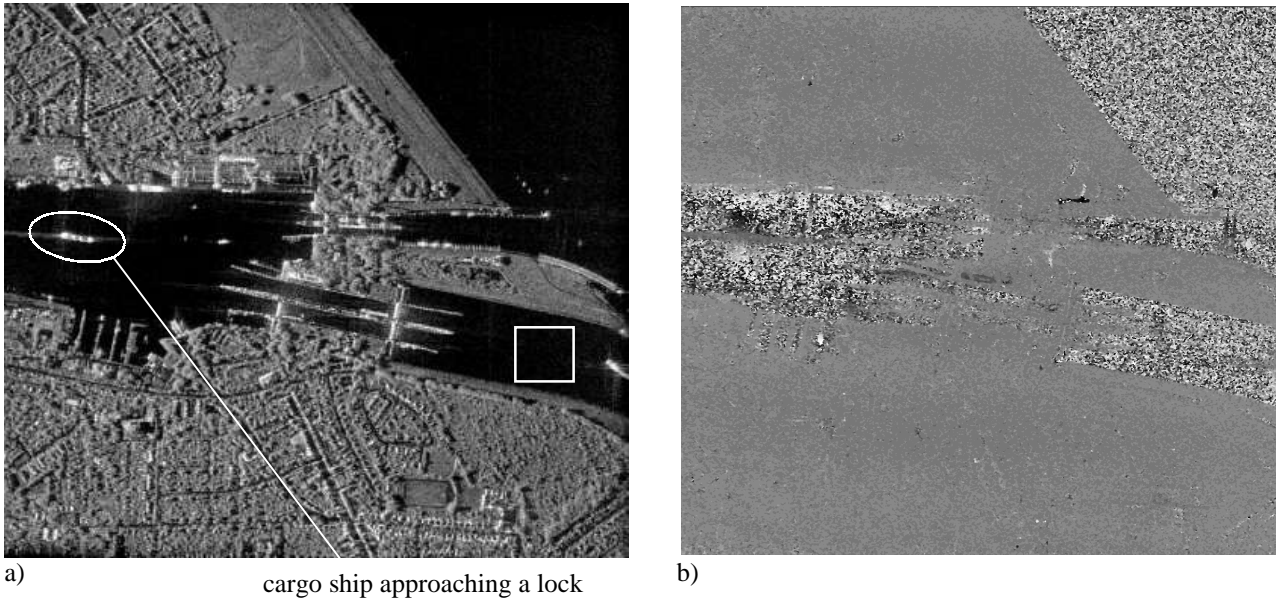


Figure 4: along-track interferometry a) intensity image, the scene show inland waterways in the vicinity of lock with incoming and leaving cargo ships b) corresponding phase differences as gray scale image

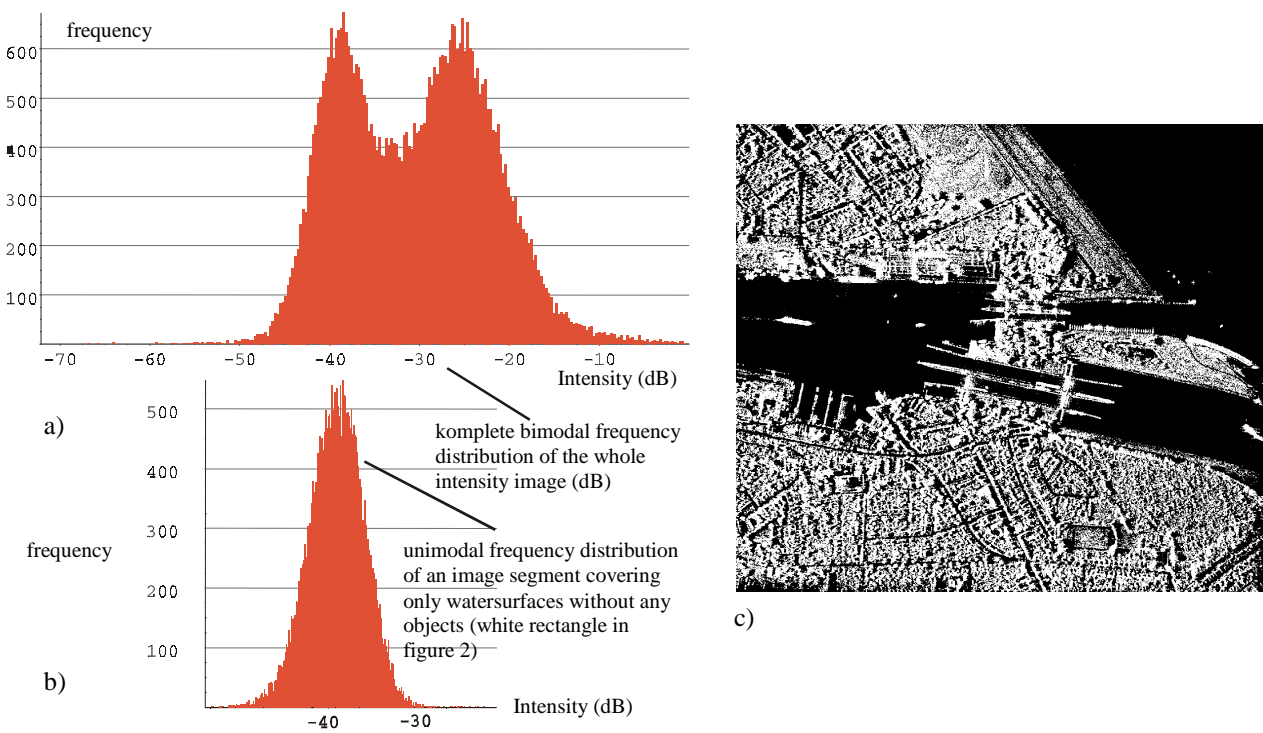


Figure 5: a) Bimodal frequency distribution of the intensity image (dB)  
 b) Unimodal frequency distribution of an image segment covering only water surface without any objects, the considered image segment corresponds to the white square in figure 2a).  
 c) Binary mask extracted from intensity image

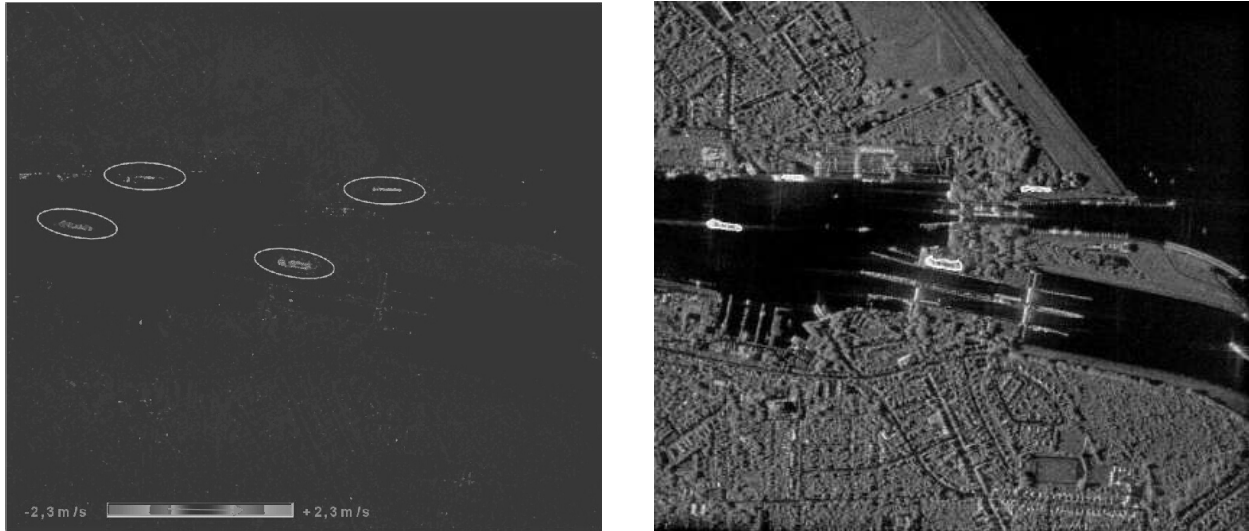


Figure 6: a) masked velocities (phase differences) and b) segmented moving objects

#### 4. RESULTS

The test data set shows a scene in the vicinity of a lock. On the waterway are several cargo ships present, which are just entering or leaving the lock area. Figure 3 gives an overview of the test side. Three cargo ships could be identified. In the upper lock a cargo ship is leaving and in the lower lock a ship is entering (Figure 3). A third ship is approaching from the left. The velocities of these cargo ships are in the range of some km/h and they are about 100 m long and 20 m wide. Figure 4 shows the intensity image and the phase differences. In the intensity image the ships are difficult to detect because of the azimuth displacement. An unfavorable consequence of the azimuth displacement can be, that the ships are not located on the waterways anymore. Figure 7 shows an significant example. Although the cargo ship is slowly moving into the lock, its displacement is so strong, that the apparent position in the SAR intensity image is completely at the land.

Because of the distortion by the noise, the position of the ships in the phase image are also difficult to identify. The phase image was masked by binary mask derived from intensity image. All values with lower intensities as 27dB were masked. Figure 5c shows the binary mask which mainly separates the water ways from the land. By a simple multiplication of the binary image with the velocity field derived by the phase differences we get the image shown in Figure 6a. The region growing process is started in the masked phase image and results in more than 700 extracted region objects. The Figure 6b shows the result of the selection process of the applied rule system. At the end 4 region objects were identified as hypotheses for cargo ships. For each region a mean velocity was calculated by the weighted average of the single velocities included by the extracted object contours. Because of the fact that we have a visible image - acquired at the same time like the SAR images - it is a quite favorable opportunity to estimate the velocities of the ships by measuring the displacement distance  $\Delta r_{\text{displ}}$  in the intensity image. If the object motion is smooth, object image will be displaced in cross-range [20] by

$$\Delta r_{\text{displ}} = \frac{R}{V} \cdot v_{\text{los}}, \quad (4)$$

where  $v_{\text{los}}$  is the radial (line of sight) velocity component of the moving object. The ships close to the canal or lock borders could be identified in the SAR intensity images and in the visible image, so that relatively good estimate of the displacement  $\Delta r_{\text{displ}}$  was possible. For the ship depicted in Figure 7 we achieve a ground velocity of 3.4 km/h by the evaluation of the azimuth displacement. The mean velocity calculated by equation (2) with the weighted average phase difference leads to a smaller value of 2.9 km/h, but both values lies in the estimated mutual uncertainty intervals. All ships marked in Figure 3 were segmented and detected. But also one ship which seems to be anchored at the upper canal side is marked and seems to have a velocity not equal to zero. This result is probably caused from double bouncing effects together with the quay or from ship movements due to bow waves. A single ship at the right border of the image was not segmented, but in this case the phase differences over the ship surface did not lead to an unambiguous velocity, possibly because of a turning movement.

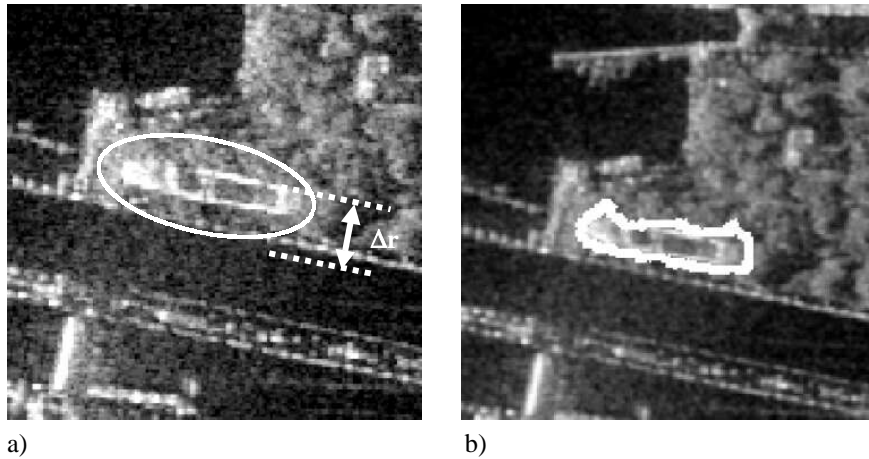


Figure 7: a) Intensity image detail, showing the displacement of a cargo ship slowly entering the lock  
 b) Segmentation result of a) with the border of extracted cargo ship

## 5. CONCLUSION

The presented approach of a combined evaluation of intensity and phase information shows promising first results for a detection and velocity estimation for single objects located at the ground or water surface. All objects in the scenery matching the model parameters were segmented. For one of the objects a rough estimate of the object velocity by the azimuth displacement shows a sufficient agreement with the measurement results based on the evaluation of the phase difference. For the present, the method is limited to tasks for which the implemented simple model is discriminating, but with the steadily increasing quality of the available SAR data this techniques seems to offer a broad potential for further applications.

## ACKNOWLEDGMENTS

We want to thank Dr. Ender (FGAN-FHR Research Institute for High Frequency Physics and Radar Techniques) for providing us the InSAR image data. The data were recorded by the AER-II experimental system of FGAN.

## 6. REFERENCES

1. M. DeFazio, F. Vinelli, "DEM Reconstruction in SAR interferometry: practical experiences with ERS-1 SAR data", IGARSS 93, vol., pp. 1207-1209, 1993.
2. P. Santitamnont, "Interferometric SAR Processing for Topographic Mapping", Dissertation Nr. 230, Wissenschaftliche Arbeiten der Fachrichtung Vermessungswesen der Universität Hannover, ISSN 0174-1454, Hannover, 1998.
3. R. Scheiber, A. Ulbricht, A. Reigber, K. P. Papathanassiou, A. Moreira, "Airborne Interferometric SAR Activities in DLR", RTO Research and Technology Organization Meeting in Granada Spain, RTO-MP-Proceeding no. 40, pp. 68.1-68.10, March, 1999.
4. R. M. Goldstein, H. A. Zebker, "Interferometric Radar Measurements of Ocean Surface Currents", Nature vol. 328, pp. 707-709, August, 1987.
5. P. W. Vachon, J. W. M. Campbell, A. L. Gray, F. Dobson, „Validation of Along-Track Interferometric SAR Measurements of Ocean Surface Waves“, IEEE Transaction on Geoscience and Remote Sensing, vol. 37, no. 1, January, 1999.
6. R. Romeiser, D.R. Thompson, "Advanced Modeling of Microwave Doppler Spectra and Along-Track Interferometric SAR Signatures of Ocean Surface Currents", Proceedings of IGARSS, Hamburg, Germany, vol. 5, pp. 2604-2606 July, 1999.

7. H. Greidanus, R.J.P. Van Bree, E.J. Husing, J. Vogelzang, E.M.J. Vaessen, "Coastal Currents with Along-Track Interferometry", Proceedings of IGARSS, Hamburg, Germany, vol. 5, pp. 2607-2609, July, 1999.
8. J. S. Lee, P. Papathanasiou, T. L. Ainsworth, M. R. Grunes, A. Reigber, "A New Technique for Noise Filtering of SAR Interferometric Phase Images", IEEE Transactions on Geoscience and Remote Sensing, Vol. 36, No. 5, p. 1456-1465, 1998.
9. J. S. Lee, K. W. Hoppel, S.A. Mange, A. R. Miller, "Intensity and Phase Statistics of Multilook Polarimetric and Interferometric SAR Imagery", IEEE Transactions on Geoscience and Remote Sensing, vol. 32, no. 5, pp. 1017-1028, 1994.
10. M. Walessa, M. Datcu, "Enhancement of Interferometric DEMs by Spatially Adaptive Model-Based Filtering in Non-Stationary Noise", Proceedings of EUSAR 2000, S. 695-698, 2000.
11. C. H. Chen (Ed.), Information Processing for Remote Sensing, World Scientific Publishing, ISBN 981-02-3737-5, Singapore, 1999.
12. U. Stilla, E. Michaelsen, "Semantic Modelling of Man-Made Objects by Production Nets", In: A. Gruen, E. P. Baltasvias, O. Henricsson (eds) Automatic Extraction of Man-made Objects from Aerial and Space Images (II). Basel: Birkhäuser, pp. 43-52, 1997.
13. U. Stilla, E. Michaelsen, K. Lütjen, "Automatic extraction of buildings from aerial images", Mapping buildings, roads and other man-made structures from images, F. Leberl, R. Kalliany, M. Gruber (eds), Wien, Oldenburg, pp. 229-244, 1996.
14. U. Soergel, K. Schulz, U. Thoennessen, "Segmentation of interferometric SAR in urban areas", Proceeding of the SPIE 15<sup>th</sup> AeroSense Symposium, April, 2001.
15. U. Soergel, U. Thoennessen, H. Gross and U. Stilla, "Segmentation of Interferometric SAR Data for Building Detection", IAPRS, Vol. 23, Amsterdam, 2000.
16. J. H. G. Ender, "Experimental Results Achieved with the Airborne Multi-Channel SAR System AER-II". Proceedings of EUSAR'98, VDE-Verlag, ISBN 3-8007-2359-x, Friedrichshafen, Germany, p. 315-318, 1998.
17. P. Berens, "Spotlight SAR with an electronical steered beam - experimental results achieved with the airborne AER-II", Proceeding of IRS'98, Munich, Germany, pp. 1353-1360, 1998.
18. R. Scheiber, K. P. Papathanassiou, A. Moreira, "Along-Track-Interferometry Using a Modified Polarimetric SAR System", Proceeding of the EUSAR'98, pp. 587-590, May, 1998.
19. R. Scheiber, A. Ulbricht, A. Reigber, K. P. Papathanassiou, A. Moreira, "Airborne Interferometric SAR Activities in DLR", RTO Research and Technology Organization Meeting in Granada Spain, RTO-MP-Proceeding no. 40, pp. 68.1-68.10, March, 1998.
20. R. J. Sullivan, Microwave radar: imaging and advanced concepts, Artech House Inc., London, ISBN 0-89006-341-9, 2000.